ABSTRACT

Materials with negative elastic moduli are unstable, but can be stabilised by specific boundary conditions. In particulate materials under compression, rotating non-spherical particles produce the effect of negative Cosserat shear modulus. We consider wave propagation in such materials and demonstrate that when the sum of the negative Cosserat shear modulus and the conventional shear modulus is positive the waves can propagate. In the conventional isotropic Cosserat continuum the twist wave and one of the shear waves exist only at frequencies higher than a threshold. When the Cosserat shear modulus is negative all waves exist at all frequencies; observing the twist and shear waves one can detect and investigate the negative moduli.

1   Introduction

Positive definiteness of the elastic potential energy is a thermodynamic requirement. It also ensures the uniqueness of elastic solution and, consequently, the stability of the corresponding material or the system. This imposes certain conditions on the values of the elastic constants. For instance in isotropic elasticity, the condition of positive definiteness imposes the following condition on the bulk and shear moduli, $\kappa > 0$, $\mu > 0$ (Landau & Lifshitz, 1986), while the first Lame constant can be negative, as long as $\lambda > -2\mu/3$. This also includes negative Poisson's ratio (see for instance Pasternak and Dyskin, 2012a and the literature review therein), as long it is greater than -1.

In what follows the term *negative stiffness* will explicitly refer to the cases when the negative values of the corresponding moduli do violate the positive definiteness of the energy. For example, if a spring with negative stiffness is loaded, the loading device does work on loading while the elastic energy reduces. This contradiction manifests itself in instability of such a system. Nevertheless the negative stiffness systems or materials can still be stable in a certain range of values of negative stiffness if the stability is maintained by appropriate boundary conditions (Dyskin & Pasternak, 2012a, 2012b; Kochmann & Milton, 2014). Thereafter we only consider the case when the stability is maintained by the appropriate boundary conditions. This paper does not consider the metamaterials in which peculiarities of wave propagation such as the presence of wave bands are interpreted in terms of negative dynamic modulus (Cheng, Xu, & Liu, 2008; Ding, Liu, Qiu, & Shi, 2007; Fang et al., 2006; Lee, Park, Seo, Wang, & Kim, 2009; Morvan, Tinel, Hladky-Hennion, Vasseur, & Dubus, 2010), negative mass/density (Ding et al., 2007; Park, Park, Lee, & Lee, 2015) or negative refraction index (Guenneau, Movchan, Petursson, & Ramakrishna, 2007; Lee, Ma, Lee, Kim, & Kim, 2011). A notion was put forward of a possibility of breakage of the second law of thermodynamics at very small scale and very short times, see (Ostoja-Starzewski &

Malyarenko, 2014) for details. Notwithstanding this possibility we consider a macroscopic (effective) negative stiffness that can be exhibited by some structures.

We base our consideration on the fact that a number of mechanisms and material elements have been found to exhibit negative stiffness in a certain range of magnitudes of the loading and under appropriate boundary conditions. An obvious example is the post-peak softening of the rocks and concrete where the stability is clearly controlled by the stiffness of the loading device, that is by the boundary conditions (Cook, 1965; Salamon, 1970; Tarasov & Dyskin, 2005). Systems with negative stiffness include systems of elastic springs, arches, links and certain link and lever mechanisms (Carrella, Brennan, & Waters, 2008; Champneys, Hunt, & Thompson, 1999; Hunt, Muhlhaus, & Whiting, 1997; Park & Luu, 2007; Thompson & Hunt, 1973; Wang & Lakes, 2004). Negative shear modulus is exhibited by a cell comprised of four masses mutually connected by pre-loaded elastic springs of different stiffnesses (Lakes & Drugan, 2002). Tubes and columns pre-buckled to an S-shaped configuration (Bažant & Cedolin, 1991; Lakes, 2001) and nanotubes (Yap, Lakes, & Carpick, 2008) show negative stiffness. Negative stiffness is observed in single foam cells (Lakes, Rosakis, & Ruina, 1993) and was recently detected in hair-bundles in the ear: the negative stiffness is believed to be the basis of an amplification mechanism in hearing (Martin, Mehta, & Hudspeth, 2000). Phase transformations can produce an effect of negative stiffness (Roytburd, 1996). Rotating levers give another example of a mechanism producing negative stiffness (Tarasov & Randolph, 2008). Plate-like interlocking structures of cubic elements constrained by a rigid frame show negative stiffness in the post-peak stage (Estrin et al., 2004; Schaare et al., 2008).

Recently, the first two authors proposed yet another mechanism of apparent negative stiffness based on rotation of non-spherical particles, Fig. 1a (Dyskin & Pasternak, 2011, 2012b, 2012c). The effect is apparent from the consideration of moment equilibrium about the point of particle contact. The particle rotation is resisted by compressive load P that creates a moment balancing the moment from the shear force. Subsequently, as the particle rotates the arm of application of the compressive force reduces thus reducing the resisting moment, Fig. 1b. The importance of this mechanism is in its ubiquity: it can work in granular materials as well as in rocks at different scales (Dyskin and Pasternak 2012c) and concrete at advanced stages of loading when the accumulated damage leads to grain/aggregate detachment enabling their independent rotation. (We note that modelling of granular materials, rocks and concrete is usually conducted under the assumption that the grains are spherical, which erases the effect of negative stiffness.) Furthermore, the considered negative stiffness mechanism is reversible: the reduction of the displacement causes increase in the shear force.

According to (Dyskin & Pasternak, 2011, 2012b, 2012c) the infinitesimal dependence between the displacement and force is given by

$$dT = kdu; \ k = -\frac{P}{d\sin^3\theta} \tag{1}$$

This dependence is characterised by a negative stiffness, $k < 0$. Subsequently, the rotating non-spherical particle gives an example of a simplest system with structural negative stiffness.

Relationship (1) between the shear force, T, and shear displacement, u, was interpreted in (Dyskin & Pasternak, 2011, 2012b, 2012c) as the effect of negative shear modulus. We note however, that the mechanism of such a relationship is in the rotation of the (non-spherical) grain. We now rewrite this relationship in terms of shear force, T, vs. the grain rotation angle, φ. It reads

$$dT = k'd\varphi; \ k' = -\frac{P}{\sin^3 \theta} \tag{2}$$

We see that stiffness k' (it has dimensions of force, which is different from the dimensions of k) relating the shear force and rotation is negative. This brings us to the notion of negative Cosserat shear modulus, the modulus that relates the non-symmetrical part of the Cosserat stress tensor and the Cosserat rotations.
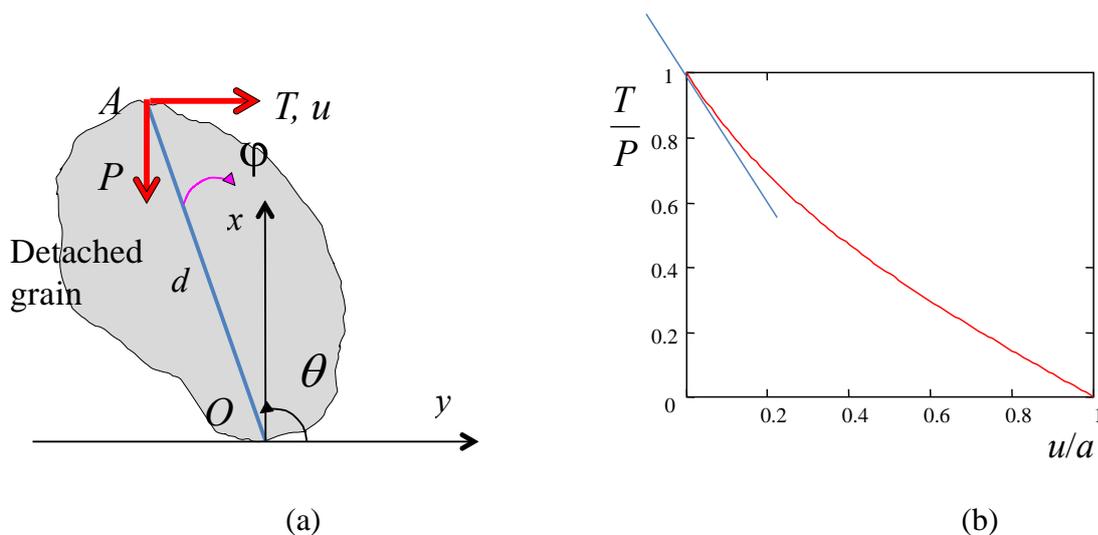

(a)   (b)

Fig. 1. Apparent negative stiffness (the factor relating T and u) produced by rotation of a non-spherical grain: (a) rotating grain; (b) relation between normalised shear force and displacement.

While formally relating the tangential force and displacement, Figure 1b, this mechanism involves independent grain rotation that constitutes an additional (rotational) degree of freedom. In continuum modelling this corresponds to the appearance of the vector field of rotations independent of the vector field of displacements such that each point has 6 degrees of freedom (three translational and three rotational). This requires the use of the Cosserat theory for its description. The above effect of negative stiffness concerns the relation between the non-symmetric part of the shear stress (observe the non-symmetry of the shear force

shown in Fig. 1a) and the (independent) rotation. This type of relation is controlled by what is called the Cosserat shear modulus, which can now be negative. Furthermore, Fig. 1 provides a simple example of a structure which when stabilised (that is undergoes displacement-controlled loading) exhibits negative Cosserat shear modulus. The present paper considers the effect of negative Cosserat shear modulus on wave propagation in isotropic Cosserat continuum.

2 Isotropic Cosserat continuum

As mentioned above, modelling materials with independent internal rotations (e.g., rotating particles) requires the introduction of a Cosserat continuum whereby the internal rotations add three more degrees of freedom on top of three classical ones associated with displacements. This isotropic formulation is the simplest theory that relates independent rotations and shear stress and that is the reason why we have chosen it from numerous other high order formulations. Subsequently, the presence of rotations calls for a set of deformation measures richer than in the classical continuum. These are strain and curvature-twist tensors defined as (e.g. Nowacki, 1970):

$$\gamma_{ji} = u_{i,j} - \varepsilon_{kji}\varphi_k; \quad \kappa_{ji} = \varphi_{i,j} \tag{3}$$

where φ_k is the rotation vector. One can see that the new strain tensor, γ_{ji}, is non-symmetric; its non-diagonal components include both displacement gradients and the components of the vector of internal rotations. The symmetrical part of the Cosserat strain tensor gives the classical strain tensor. On top of that an additional deformation measure is introduced, the curvature-twist tensor, κ_{ji}, which is the tensor of rotation gradients.

The reciprocal quantities are the non-symmetric stress tensor, σ_{ij}, and moment stress tensor, μ_{ij}, which combine forces and moments per unit area of the faces of the corresponding volume element. The Cosserat equations of motion read:

$$\begin{aligned} \sigma_{ji,j} &= \rho\ddot{u}_i \\ \mu_{ji,j} + \varepsilon_{kji}\sigma_{jk} &= J\ddot{\varphi}_i \end{aligned} \tag{4}$$

where ρ is the material density, J is the density of inertia moment. Here, the body forces and body moments are neglected.

The Hooke's law for isotropic Cosserat continuum can be expressed as (e.g., Nowacki, 1970):

$$\sigma_{ji} = (\mu+\alpha)\gamma_{ji} + (\mu-\alpha)\gamma_{ij} + \lambda\gamma_{kk}\delta_{ij} \tag{5}$$

$$\mu_{ji} = (\gamma+\varepsilon)\kappa_{ji} + (\gamma-\varepsilon)\kappa_{ij} + \beta\kappa_{kk}\delta_{ij} \tag{6}$$

where λ and μ are the Lame constants, α is the shear Cosserat modulus, γ, ε, β are the Cosserat moduli.

In order to find the conditions of stability of isotropic Cosserat continuum consider the strain energy density for the isotropic Cosserat continuum as a function of relative deformations γ_{ij} and twist-curvatures κ_{ij}. In the absence of thermal components the strain energy density is expressed as (e.g., Nowacki, 1970):

$$W = \frac{\mu+\alpha}{2}\gamma_{ji}\gamma_{ji} + \frac{\mu-\alpha}{2}\gamma_{ji}\gamma_{ij} + \frac{\lambda}{2}\gamma_{kk}\gamma_{nn} + \frac{\gamma+\varepsilon}{2}\kappa_{ji}\kappa_{ji} + \frac{\gamma-\varepsilon}{2}\kappa_{ji}\kappa_{ij} + \frac{\beta}{2}\kappa_{kk}\kappa_{nn} \qquad (7)$$

We rewrite this representation in the following form:

$$\begin{aligned}
W = &\frac{\mu}{2}\gamma_{(ji)}\gamma_{(ji)} + \frac{\alpha}{2}\gamma_{\langle ji\rangle}\gamma_{\langle ij\rangle} - \frac{\mu+\alpha}{4}\gamma_{(ji)}\gamma_{\langle ji\rangle} + \frac{\lambda}{2}\gamma_{kk}\gamma_{nn} \\
&+ \frac{\gamma}{2}\kappa_{(ji)}\kappa_{(ji)} + \frac{\varepsilon}{2}\kappa_{\langle ji\rangle}\kappa_{\langle ij\rangle} - \frac{\gamma+\varepsilon}{4}\kappa_{(ji)}\kappa_{\langle ji\rangle} + \frac{\beta}{2}\kappa_{kk}\kappa_{nn}
\end{aligned} \qquad (8)$$

Here

$$\gamma_{(ij)} = \frac{1}{2}\left(\gamma_{ij}+\gamma_{ji}\right), \quad \gamma_{\langle ij\rangle} = \frac{1}{2}\left(\gamma_{ij}-\gamma_{ji}\right), \quad \kappa_{(ij)} = \frac{1}{2}\left(\kappa_{ij}+\kappa_{ji}\right), \quad \kappa_{\langle ij\rangle} = \frac{1}{2}\left(\kappa_{ij}-\kappa_{ji}\right) \qquad (9)$$

are the symmetric and antisymmetric parts of strain and curvature twist tensors respectively. It is important that the antisymmetric parts are independent from both the symmetric parts and the traces (γ_{nn} and κ_{nn}). It is clear from (9) that if $\alpha \leq 0$, the energy is not positive definite. (Indeed, if $\alpha \leq 0$ then by choosing the deformation with $\gamma_{(ij)}$ and κ equal to zero one has $W = \left(\alpha/2\right)\gamma_{\langle ji\rangle}\gamma_{\langle ij\rangle} \leq 0$).

Now we see that the thermodynamics requires that $\alpha > 0$. The case we attempt to consider, $\alpha < 0$, which is thermodynamically inadmissible (yet structures with apparent negative stiffness do exist, see Introduction). We interpret this in the sense that an isotropic material with negative Cosserat shear modulus can exist (be stable), but only under certain boundary conditions (or, more generally as a part of an encompassing mechanical system such that the total energy of the material + system is positive definite, Dyskin and Pasternak, 2012).

In what follows we consider an infinite solid with $\alpha < 0$ assuming that at infinity the applied boundary conditions are such that the solid is stable. We now consider planar waves in such a solid propagating along an x_1 axis and determine the types and velocity of the waves. For a conventional Cosserat continuum the types and velocity of planar waves are known (e.g., Nowacki, 1970): there are a pressure wave, two shear waves (we will later see that they are in fact shear-rotational waves (Pasternak, 2002; Pasternak & Muhlhaus, 2005), since they involve both displacements and rotations) and a twist wave, all waves except the pressure wave show dispersion (the dependence of the wave velocity upon frequency). The following

chapter will introduce the expressions for the wave velocities in the conventional isotropic Cosserat continuum and then generalise them to the case of negative Cosserat shear modulus.

3 Planar waves

3.1. Planar waves in conventional isotropic Cosserat continuum

The dynamic equations of motion with respect to displacement and rotation vectors are obtained by substituting the constitutive equations (5), (6) into the equations of motion (4). It is convenient to write, following (Nowacki, 1970), the obtained equation in the vector form. Neglecting the temperature variations caused by deformation the equations of motion can be expressed as:

$$\begin{aligned}
(\lambda + 2\mu)\,\text{grad}\,\text{div}\mathbf{u} - (\mu + \alpha)\,\text{rot}\,\text{rot}\mathbf{u} + 2\alpha\,\text{rot}\boldsymbol{\varphi} = \rho\ddot{\mathbf{u}} \\
(\beta + 2\gamma)\,\text{grad}\,\text{div}\boldsymbol{\varphi} - (\gamma + \varepsilon)\,\text{rot}\,\text{rot}\boldsymbol{\varphi} + 2\alpha\,\text{rot}\mathbf{u} = \rho\ddot{\boldsymbol{\varphi}}
\end{aligned} \tag{10}$$

Representing the displacement and rotation vectors, $\mathbf{u}$, $\boldsymbol{\varphi}$ through scalar and vector potentials, Ψ, $\mathbf{H}$:

$$\begin{aligned}
\mathbf{u} = \text{grad}\,\Phi + \text{rot}\,\Psi, \quad \text{div}\Psi = 0 \\
\boldsymbol{\varphi} = \text{grad}\,\Sigma + \text{rot}\,\mathbf{H}, \quad \text{div}\mathbf{H} = 0
\end{aligned} \tag{11}$$

and directing the x_1 axis along the direction of propagation of the planar wave such that the displacement, rotation and potentials are the functions of x_1 only, one obtains the following wave equations with respect to the potentials (Nowacki, 1970):

$$\Box_1 \Phi = 0, \quad \Box_3 \Sigma = 0, \quad \Omega\Psi = 0, \quad \Omega\mathbf{H} = 0 \tag{12}$$

where the differential operators in (12) have the following form:

$$\begin{aligned}
\Box_1 = (\lambda + 2\mu)\nabla^2 - \rho\partial_t^2, \quad \Box_3 = (\beta + 2\gamma)\nabla^2 - 4\alpha - J\partial_t^2 \\
\Box_2 = (\mu + \alpha)\nabla^2 - \rho\partial_t^2, \quad \Box_4 = (\gamma + \varepsilon)\nabla^2 - 4\alpha - J\partial_t^2 \\
\Omega = \Box_2\Box_4 + 4\alpha^2\nabla^2
\end{aligned} \tag{13}$$

It is seen that equations (10) get reduced to 4 separate equations with respect to potentials, Φ, Σ, Ψ and $\mathbf{H}$. Furthermore, equations for Ψ and $\mathbf{H}$ have identical form. Now we can count the wave types. The first two waves are given by:

$$\mathbf{u} = \text{grad}\,\Phi, \quad \boldsymbol{\varphi} = \text{grad}\,\Sigma \tag{14}$$

The first one is the wave with displacement vector parallel to the direction of wave propagation. This is the familiar *p-wave* (*pressure wave*). Another wave is the wave with rotation vector parallel to the direction of wave propagation. This is what is called the *twist wave* as the rotation proceeds about axis parallel to the direction of wave propagation.

The other two types of waves are given by:

$$\mathbf{u} = \operatorname{rot} \mathbf{\Psi}, \quad \boldsymbol{\varphi} = \operatorname{rot} \mathbf{H} \tag{15}$$

These are waves with displacement and rotation vectors normal to the direction of wave propagation. The waves with displacement vectors normal to the direction of wave propagation are known as shear waves. However, since both waves are governed by equations having the same form (the last two equations in (12)) their velocities coincide. That is the reason for merging them into the same type and call them the *shear-rotational waves* (Pasternak, 2002; Pasternak & Muhlhaus, 2005). (In Nowacki, 1970, these waves are referred to as shear waves. We find this terminology confusing as it ignores the rotational part of the waves.)

Now we find the wave velocities assuming that the waves are monochromic and following (Nowacki, 1970). We assume the potentials in the form:

$$\Phi = A \exp\left(-i\omega t + ikx_1\right), \quad \mathbf{\Sigma} = \mathbf{B} \exp\left(-i\omega t + ikx_1\right)$$
$$\mathbf{\Psi} = C \exp\left(-i\omega t + ikx_1\right), \quad \mathbf{H} = \mathbf{D} \exp\left(-i\omega t + ikx_1\right) \tag{16}$$

where ω is the frequency.

Substituting (16) into (12) one obtains three characteristic equations for the wave number k (equations obtained using $\mathbf{\Psi}$ and $\mathbf{H}$ coincide).

The first equation is equation for the *p*-wave (*pressure wave*) in which the materials points oscillate in the direction coinciding with the direction of wave propagation. The velocity, c_1, turns out to be the same as in the classical continuum:

$$c_1^2 = \frac{\lambda + 2\mu}{\rho} \tag{17}$$

Isotropic Cosserat continuum produces two dispersional shear-rotational waves. They involve the displacement and rotation of the material points in the directions normal to the direction of wave propagation). Their velocities are derivable from the wave number given by the following characteristic equation (Nowacki, 1970) common for the shear and rotational components:

$$c_2^2 c_4^2 k^4 + \left[\omega_*^2 c_5^2 - \omega^2 \left(c_2^2 + c_4^2\right)\right] k^2 - \omega^2 \left(\omega_*^2 - \omega^2\right) = 0 \tag{18}$$

Here $c_2^2 = (\mu + \alpha)/\rho$, $c_4^2 = (\gamma + \varepsilon)/J$, $c_5^2 = \mu/\rho$, k is the wave number, ω is the frequency and

$$\omega_*^2 = \frac{4\alpha}{J}, \quad c_3^2 = \frac{\beta + 2\gamma}{J} \tag{19}$$

Frequency ω_* is a threshold frequency: when $\omega < \omega_*$ only one shear-rotational wave exists (eq. (18) has only one real solution). Its velocity tends to the velocity of the classical shear wave as frequency tends to zero. When $\omega > \omega_*$ the second shear-rotational wave (second real solution of eq. (18)) appears.

For the following it is convenient to rewrite (19) in a dimensionless form. To this end we introduce the dimensionless groups (similar to the ones introduced in (Pasternak & Dyskin, 2010; Pasternak & Dyskin, 2014)):

$$s_5 = \frac{c_s^2}{c_5^2} = \frac{\omega^2}{k^2 c_5^2}, \quad s_2 = \frac{c_2^2}{c_5^2} = 1 + \frac{\alpha}{\mu},$$

$$s_4 = \frac{c_4^2}{c_5^2} = \frac{(\gamma + \varepsilon)\rho}{J\mu}, \quad w = \frac{\omega_*^2}{\omega^2} = \frac{4\alpha}{J\omega^2} = z\frac{\alpha}{\mu}, \quad z = \frac{4\mu}{J\omega^2}$$

(20)

Subsequently, in the dimensionless form equation (18) reads:

$$(w-1)s^2 + \left[w - (s_2 + s_4)\right]s - s_2 s_4 = 0,$$

or

$$\left(z\frac{\alpha}{\mu} - 1\right)s^2 - \left[z\frac{\alpha}{\mu} - \left(1 + \frac{\alpha}{\mu} + s_4\right)\right]s - \left(1 + \frac{\alpha}{\mu}\right)s_4 = 0,$$

(21)

The fourth wave type is the twist wave which involves rotations around the direction of wave propagation (the rotation vector coincides with the x_1 axis). For the frequencies higher than the threshold frequency, $\omega > \omega_*$, the twist wave velocity in the isotropic Cosserat continuum is:

$$c_t = \frac{c_3}{\sqrt{1 - \left(\dfrac{\omega_*}{\omega}\right)^2}}$$

(22)

This relationship is shown in Figure 2a. It is seen that as frequency $\omega \to \omega_* + 0$ the wave velocity tends to infinity.

3.2. Planar waves in the presence of negative Cosserat shear modulus

We now consider the case of negative Cosserat shear modulus, α<0. We introduce the following notations:

$$\alpha = -\alpha_n, \quad \omega_*^2 = -\frac{4\alpha_n}{J}, \quad \omega_n^2 = -\omega_*^2$$

(23)

It can be seen that Eq. (17) for velocity c_1 of the p-wave does not depend on α and will therefore not change:

Equation (22) for velocity c_t of the twist wave will change:

$$c_t = \frac{c_3}{\sqrt{1+\left(\dfrac{\omega_n}{\omega}\right)^2}} \tag{24}$$

The first unusual result of the presence of negative Cosserat shear modulus is the disappearance of the threshold frequency. Instead, the dispersion relation is controlled by a characteristic frequency ω_n. Now the twist waves can be generated at all frequencies, even at very low ones. This suggests a potential method of detecting the negative Cosserat shear modulus; its presence is indicated by the presence of low frequency twist waves and, as will be seen later, the second shear-rotational wave.

The dispersion relationship for the twist wave for $\alpha < 0$ is shown in Figure 2b. It is seen that the twist wave velocity reduces as frequency decreases. Furthermore, according to eq. (24), as $\omega \to 0$, the twist wave velocity vanishes, $c_t \to 0$.

Let us now consider shear-rotational waves. In the case of negative Cosserat shear modulus, $\alpha < 0$ the corresponding characteristic equation (an analogue of characteristic Eq. (22) associated with the conventional positive Cosserat shear modulus) reads:

$$(w+1)s^2 - \left[w + (s_2 + s_4)\right]s + s_2 s_4 = 0,$$
$$\text{or} \tag{25}$$
$$\left(z\frac{\alpha_n}{\mu}+1\right)s^2 - \left[z\frac{\alpha_n}{\mu} + \left(1 - \frac{\alpha_n}{\mu} + s_4\right)\right]s + \left(1 - \frac{\alpha_n}{\mu}\right)s_4 = 0,$$

where

$$s = \frac{c_s^2}{c_5^2} = \frac{\omega^2}{k^2 c_5^2}, \quad s_2 = \frac{c_2^2}{c_5^2} = 1 - \frac{\alpha_n}{\mu}, \quad s_4 = \frac{c_4^2}{c_5^2} = \frac{(\gamma+\varepsilon)\rho}{J\mu}$$
$$c_2^2 = \frac{\mu - \alpha_n}{\rho}, \quad w = \frac{\omega_n^2}{\omega^2} = -\frac{4\alpha_n}{J\omega^2} = -z\frac{\alpha_n}{\mu}, \quad z = \frac{4\mu}{J\omega^2} \tag{26}$$

As can be seen from expression (26) for s_2 the admissible values of modulus α_n are between 0 and μ. It means that the values of negative Cosserat modulus when the waves exist and the hence material is stable are in the range $-\mu < \alpha < 0$.
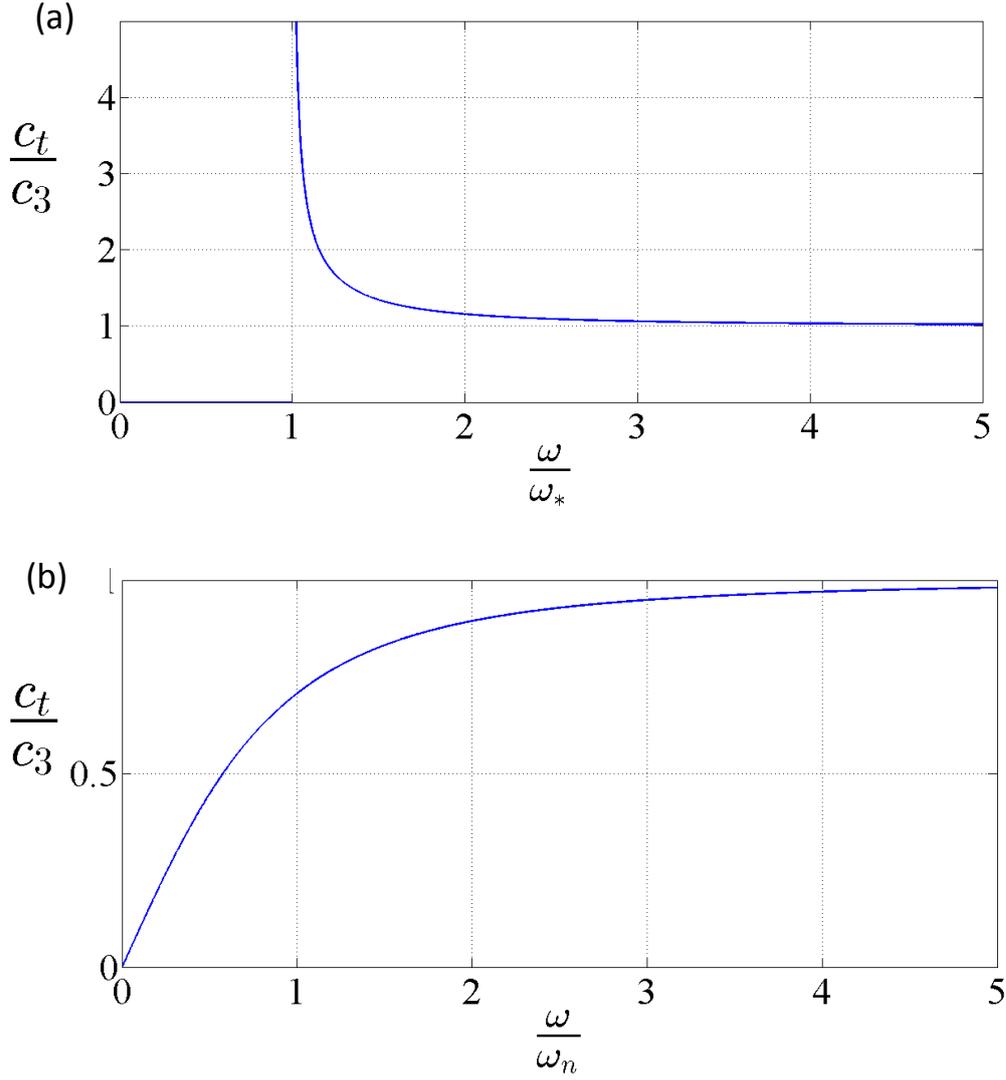
Fig. 2. Dispersion relationship for the twist wave in a Cosserat continuum: (a) with positive (α>0) and (b) with negative Cosserat shear modulus (α<0).

The dispersion relations for the shear-rotational waves for $-\mu < \alpha < 0$ are shown in Figure 3. Again, due to the absence of the threshold frequency both shear-rotational waves are present at all frequencies. It is seen that as the frequency decreases the shear-rotational wave velocities reduce. It can easily be shown from the first equation of (25) that as $\omega \to 0$, one of the shear rotational wave velocities vanishes, $c_{s1} \to 0$, while the other one tends to the velocity of a conventional shear wave, $c_{s2} \to c_5$.

Combining the solutions for both equations we find the relation between the normalised velocities of shear-rotational waves and the normalised Cosserat shear modulus α/μ, Figure 4.

As can be seen, when $z\alpha/\mu < 1$ (it means $\omega_n^2/\omega^2 < 1$, that is the frequency is greater than the controlling frequency, ω_n), we have two shear-rotational waves. This includes both the regions of negative and positive modulus α.

On the other hand, there is only one shear-rotational wave when $z\alpha/\mu > 1$ (it means $\omega_n^2/\omega^2 > 1$ that is the frequency is smaller than the controlling frequency, ω_n) and modulus α is always positive.

It is seen from Figure 4 that for the dependence of the shear-rotational wave velocities of the Cosserat shear modulus, the value $\alpha = \mu/z = 1/4\,J\omega^2$ is a discontinuity point in the relation between one of the wave velocities (the one which is highest when the Cosserat shear modulus is negative) and the Cosserat shear modulus. In order to see the physical meaning of the discontinuity we need to recall that the plots in Figure 4 correspond to a certain frequency. The value $\alpha = \mu/z = 1/4\,J\omega^2$ of the Cosserat shear modulus is the value at which the frequency used in Figure 4 reaches the threshold after which the second shear wave appears. This manifests itself as a discontinuity.

When the Cosserat shear modulus α tends to infinity the value of the normalised velocity of this shear-rotational wave tends to the following limiting value:

$$c_s/c_5 = \sqrt{\frac{z - 1 + \sqrt{1 - 2z + 4s_4 + z^2}}{2z}} \tag{27}$$

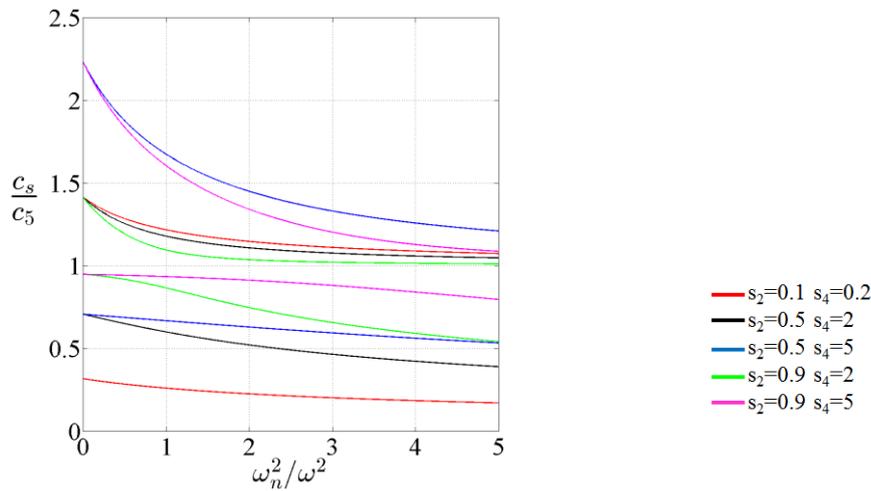**Fig. 3.** Dispersion relationships for both shear-rotational waves in a Cosserat continuum with negative Cosserat shear modulus (α<0)

4 Discussion

Dispersion relationships characteristic for shear-rotational and twist waves can be instrumental in determining parameters of the Cosserat continuum, which are not easy to

measure otherwise. A key point to it is the fact that high frequency waves in heterogeneous materials are hard to detect as the wave length should considerably exceed the microstructural length to avoid wave scattering and attenuation (e.g., Pasternak & Dyskin, 2010; Pasternak & Dyskin, 2014). Furthermore when the frequency is below the threshold only the dispersion relation of a single shear-rotational wave is accessible, which is not sufficient for the full determination of the Cosserat moduli (Pasternak & Dyskin, 2010; Pasternak & Dyskin, 2014).

The situation changes drastically when the Cosserat shear modulus is negative (but within the stability range). In this case both shear rotational waves and twist wave exist at low frequencies and hence can be detected. Furthermore, as seen in Figures 3–5, both shear-rotational waves have considerably different velocities, which potentially permits detecting them by conventional shear wave transducers utilising the difference in the arrival times (for large enough samples). This paves a way for detecting the negative stiffness effect and determining the value of the negative Cosserat shear modulus. Then using the model depicted in Figure 1 or a more sophisticated model that accounts for the resistance of the surrounding material to the dilation generated by rotations of non-spherical particles (Pasternak & Dyskin, 2013) one can analyse the mechanism of negative stiffness. Furthermore, when the rotating non-spherical constituents are used to develop hybrid materials with engineered microstructure (Pasternak, Dyskin, & Sevel, 2014) the wave measurements can be used for monitoring their state.
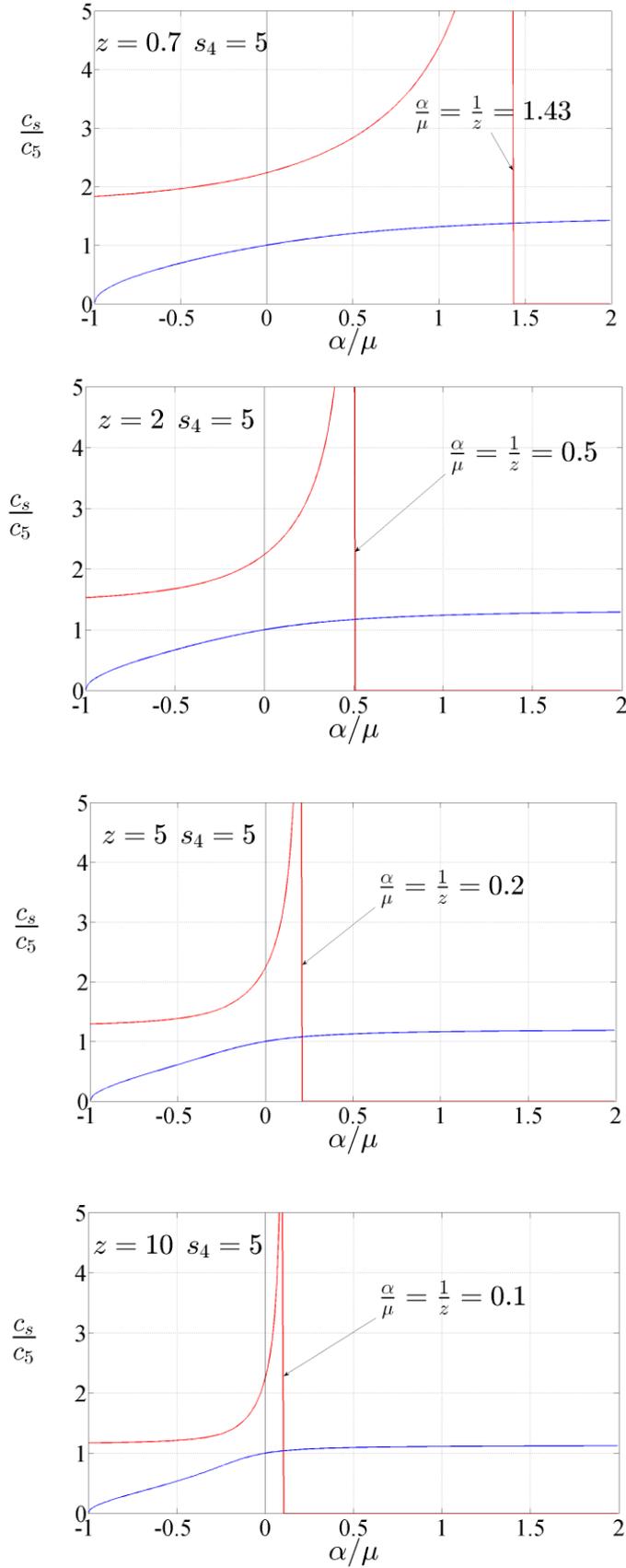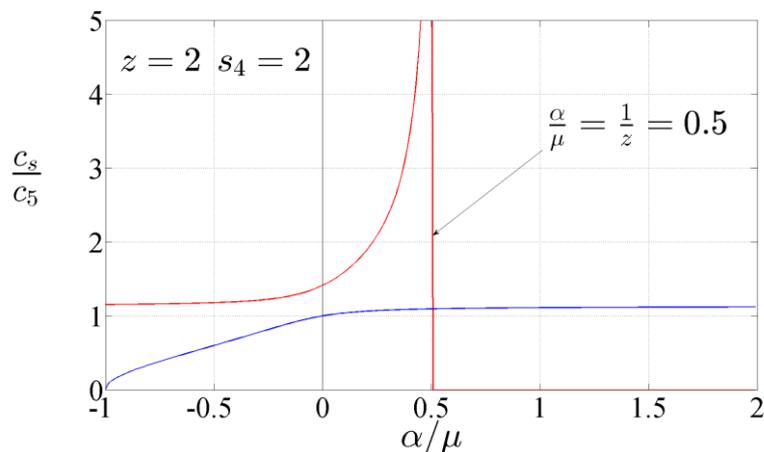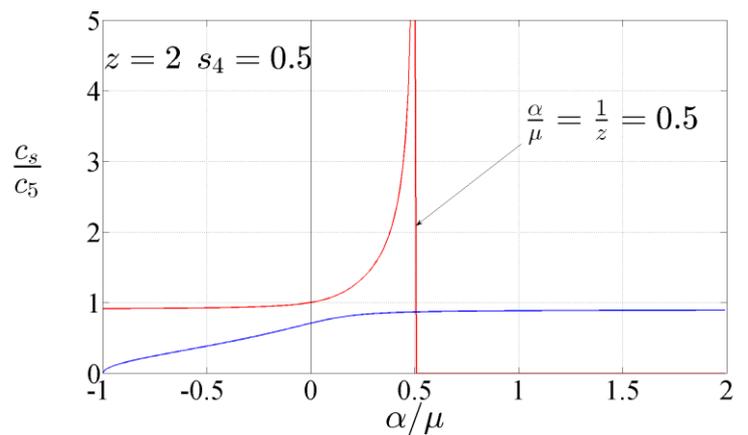
Fig. 4. Relations between normalised velocities of shear-rotational waves and normalised Cosserat shear modulus α ($z = 4\mu J^{-1}\omega^{-2}$ is varied, $s_4 = c_4^2 c_5^{-2} = 5$).

The analysis can further capitalise on the discontinuous relation between the Cosserat shear modulus and the shear-rotational wave velocities. In the cases when the Cosserat shear modulus can be varied by an external parameter, such as the magnitude of compressive load P in the example shown in Figure 1 and eq. (2) the abrupt appearance of the second shear-rotational wave (if detected) will signal the approaching transition point to the negative Cosserat shear modulus. Furthermore the velocity of the wave can be used to determine the transition point more accurately. The transition of the Cosserat shear modulus to negative values can indicate approaching instability and failure. The identification of the negative modulus effect opens a new application of the measurement of shear (shear-rotational) wave dispersion (so far the main proposed application was the determination of the moduli of conventional Cosserat continuum, e.g., Pasternak et al., 2003, Pasternak and Dyskin, 2010, 2014). The detection of the negative modulus effect and determination of its value can be used in failure monitoring for instance in geomaterials, where the instability is often associated with the presence of post-peak (softening) branch of the loading curve (Cook, 1965), which can be interpreted in terms of negative stiffness. This might revitalise the currently used microseismic methods of failure monitoring.
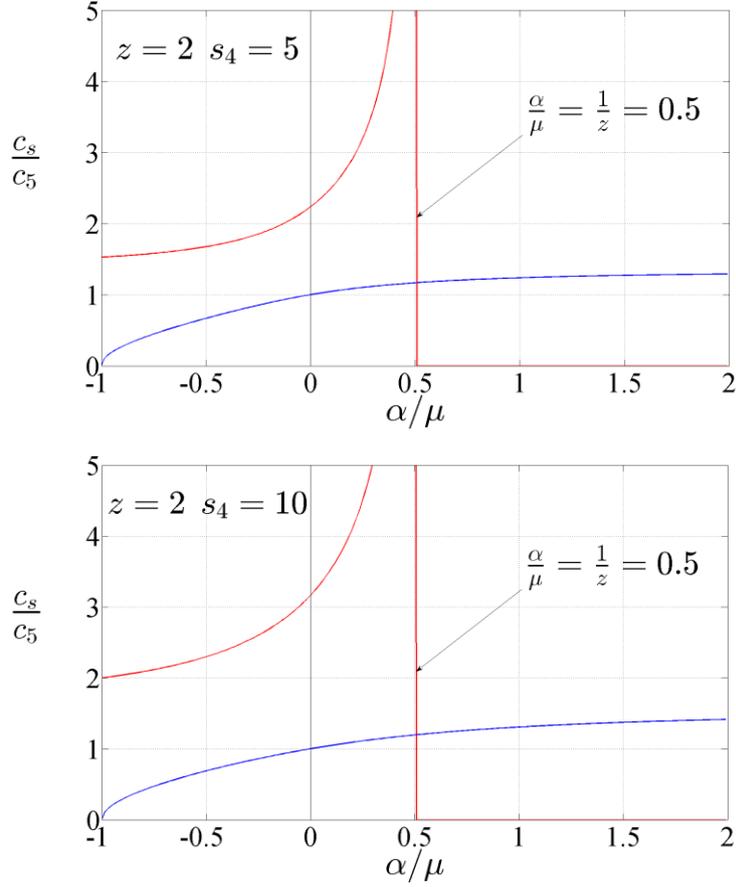
Fig. 5. Relations between normalised velocities of shear-rotational waves and normalised Cosserat shear modulus α ($s_4 = c_4^2 c_5^{-2}$ is varied, $z = 4\mu J^{-1}\omega^{-2} = 2$).

5   Conclusions

Materials with negative moduli violating the second law of thermodynamics can in some cases be stabilised by the boundary conditions or, more generally, by including them in an encompassing system such that the total energy is positive definite. In particular, in propagation of planar waves in 'infinite' isotropic Cosserat continuum (that is the waves with wavelengths much smaller than the dimensions of the material under consideration), the Cosserat shear modulus (the modulus relating the non-symmetrical part of shear stress and internal rotations) is allowed to assume negative values as long as its value does not exceed the value of the standard (positive) shear modulus. In this case the continuum still supports planar waves.

The longitudinal (*p*-wave) coincides with that of the classical continuum and hence is unaffected by the sign of the Cosserat shear modulus. For positive Cosserat shear modulus the twist wave and one of the shear-rotational waves exist only at high frequencies, higher than a certain threshold frequency, while the other shear-rotational wave exists for all

frequencies and its velocity tends to the classical shear wave velocity as the frequency tends to zero. Opposite to this, in the case of negative Cosserat shear modulus the isotropic Cosserat continuum supports the twist wave and both shear-rotational waves at all frequencies. There exists a frequency-dependent positive critical value of the Cosserat shear modulus: above this value only single shear-rotational wave exists, below this critical value the second shear-rotational wave appears with very high velocity. As the value of the Cosserat shear modulus becomes negative another wave – the twist wave appears.

The wave velocity measurements and detection of the twist wave and the second shear-rotational can provide a method of determining the Cosserat moduli and identifying the presence and measuring the value of negative Cosserat shear modulus.

6 References

Bažant, Z. P., & Cedolin, L. (1991). *Stability of structures : elastic, inelastic, fracture, and damage theories*. New York: Oxford University Press.

Carrella, A., Brennan, M. J., & Waters, T. P. (2008). Demonstrator to show the effects of negative stiffness on the natural frequency of a simple oscillator. *Proceedings of the Institution of Mechanical Engineers Part C-Journal of Mechanical Engineering Science, 222*(7), 1189-1192.

Champneys, A. R., Hunt, G. W., & Thompson, J. M. T. (1999). *Localization and solitary waves in solid mechanics*. Singapore; River Edge, N.J.: World Scientific.

Cheng, Y., Xu, J. Y., & Liu, X. J. (2008). Broad forbidden bands in parallel-coupled locally resonant ultrasonic metamaterials. *Applied Physics Letters, 92*(5).

Cook, N. G. W. (1965). The failure of rock. *International Journal of Rock Mechanics and Mining Sciences & Geomechanics Abstracts, 2*(4), 389-403.

Ding, Y., Liu, Z., Qiu, C., & Shi, J. (2007). Metamaterial with simultaneously negative bulk modulus and mass density. *Physical Review Letters, 99*(9).

Dyskin, A. V., & Pasternak, E. (2011). Friction and Localization Associated with Non-spherical Particles. In S. Bonelli, C. Dascalu, & F. Nicot (Eds.), *Advances in Bifurcation and Degradation in Geomaterials* (Vol. 11, pp. 53-58): Springer Netherlands.

Dyskin, A. V., & Pasternak, E. (2012a). Elastic composite with negative stiffness inclusions in antiplane strain. *International Journal of Engineering Science, 58*, 45-56.

Dyskin, A. V., & Pasternak, E. (2012b). Mechanical effect of rotating non-spherical particles on failure in compression. *Philosophical Magazine, 92*(28-30), 3451-3473.

Dyskin, A. V., & Pasternak, E. (2012c). Rock mass instability caused by incipient block rotation. In *Harmonising Rock Engineering and the Environment, 12th International Congress on Rock Mechanics, CRC Press / Balkema*.

Estrin, Y., Dyskin, A. V., Pasternak, E., Schaare, S., Stanchits, S., & Kanel-Belov, A. J. (2004). Negative stiffness of a layer with topologically interlocked elements. *Scripta Materialia, 50*(2), 291-294.

Fang, N., Xi, D., Xu, J., Ambati, M., Srituravanich, W., Sun, C., & Zhang, X. (2006). Ultrasonic metamaterials with negative modulus. *Nature Materials, 5*(6), 452-456.

Guenneau, S., Movchan, A., Petursson, G., & Ramakrishna, S. A. (2007). Acoustic metamaterials for sound focusing and confinement. *New Journal of Physics, 9*.

Hunt, G. W., Muhlhaus, H. B., & Whiting, A. I. M. (1997). Folding processes and solitary waves in structural geology. *Philosophical Transactions of the Royal Society a-Mathematical Physical and Engineering Sciences, 355*(1732), 2197-2213.

Kochmann, D. M., & Milton, G. W. (2014). Rigorous bounds on the effective moduli of composites and inhomogeneous bodies with negative-stiffness phases. *Journal of the Mechanics and Physics of Solids, 71*, 46-63.

Lakes, R., Rosakis, P., & Ruina, A. (1993). Microbuckling instability in elastomeric cellular solids. *Journal of Materials Science, 28*(17), 4667-4672.

Lakes, R. S. (2001). Extreme damping in compliant composites with a negative-stiffness phase. *Philosophical Magazine Letters, 81*(2), 95-100.

Lakes, R. S., & Drugan, W. J. (2002). Dramatically stiffer elastic composite materials due to a negative stiffness phase? *Journal of the Mechanics and Physics of Solids, 50*(5), 979-1009.

Landau, L. D., & Lifshitz, E. M. (1986). *Theory of elasticity*. Oxford [Oxfordshire]; New York: Pergamon Press.

Lee, M. K., Ma, P. S., Lee, I. K., Kim, H. W., & Kim, Y. Y. (2011). Negative refraction experiments with guided shear-horizontal waves in thin phononic crystal plates. *Applied Physics Letters, 98*(1).

Lee, S. H., Park, C. M., Seo, Y. M., Wang, Z. G., & Kim, C. K. (2009). Acoustic metamaterial with negative modulus. *Journal of Physics-Condensed Matter, 21*(17).

Martin, P., Mehta, A. D., & Hudspeth, A. J. (2000). Negative hair-bundle stiffness betrays a mechanism for mechanical amplification by the hair cell. *Proceedings of the National Academy of Sciences of the United States of America, 97*(22), 12026-12031.

Morvan, B., Tinel, A., Hladky-Hennion, A.-C., Vasseur, J., & Dubus, B. (2010). Experimental demonstration of the negative refraction of a transverse elastic wave in a two-dimensional solid phononic crystal. *Applied Physics Letters, 96*(10).

Nowacki, W. (1970). *Theory of micropolar elasticity. C.I.S.M.* Udine; Wien; New York: Springer.

Ostoja-Starzewski, M., & Malyarenko, A. (2014). Continuum mechanics beyond the second law of thermodynamics. *Proc Math Phys Eng Sci, 470*(2171), 20140531.

Park, J. J., Park, C. M., Lee, K. J. B., & Lee, S. H. (2015). Acoustic superlens using membrane-based metamaterials. *Applied Physics Letters, 106*(5).

Park, S. T., & Luu, T. T. (2007). Techniques for optimizing parameters of negative stiffness. *Proceedings of the Institution of Mechanical Engineers Part C-Journal of Mechanical Engineering Science, 221*(5), 505-511.

Pasternak, E. (2002). *Generalised homogenisation procedures for granular and layered materials.* (CA88404 Dr.), University of Western Australia (Australia).

Pasternak, E., & Dyskin, A. (2010). Reconstruction of Cosserat moduli in particulate materials. In M. Stavropoulou (Ed.), *Proceedings of Vardoulakis Mini-Symposia, 9th HSTAM International Congress on Mechanics* pp. 69-75. Limassol, Cyprus: University of Cyprus.

Pasternak, E. and A.V. Dyskin (2012). Materials and structures with macroscopic negative Poisson's ratio. *Intern. J. Engineering Sci.*, 52, 103-114.

Pasternak, E., & Dyskin, A. V. (2013). Instability and failure of particulate materials caused by rolling of non-spherical particles *Proceedings of the 13th International Conference on Fracture* (Vol. 1, pp. 10pp). Beijing.

Pasternak, E., & Dyskin, A. V. (2014). On a possibility of reconstruction of Cosserat moduli in particulate materials using long waves. *Acta Mechanica, 225*(8), 2409-2422.

Pasternak, E., Muhlhaus, H-B., Dyskin, A.V. (2003). Apparent Strain Localization and Shear Wave Dispersion in Elastic Fault Gouge with Microrotations, *Computational Science - ICCS 2003*, Berlin, Germany, 3, pp. 873-882.

Pasternak, E., Dyskin, A. V., & Sevel, G. (2014). Chains of oscillators with negative stiffness elements. *Journal of Sound and Vibration, 333*(24), 6676-6687.

Pasternak, E., & Muhlhaus, H. B. (2005). Generalised homogenisation procedures for granular materials. *Journal of Engineering Mathematics, 52*(1-3), 199-229.

Roytburd, A. L. (1996). Deformation through transformations. *Journal De Physique Iv, 6*(C1), 11-25.

Salamon, M. D. G. (1970). Stability, instability and design of pillar workings. *International Journal of Rock Mechanics and Mining Sciences, 7*(6), 613-&.

Schaare, S., Dyskin, A. V., Estrin, Y., Arndt, S., Pasternak, E., & Kanel-Belov, A. (2008). Point loading of assemblies of interlocked cube-shaped elements. *International Journal of Engineering Science, 46*(12), 1228-1238.

Tarasov, B. G., & Dyskin, A. V. (2005). The Phenomenon of Anomalous Rock Embrittlement. *Rasim6: Controlling Seismic Risk*, 311-317.

Tarasov, B. G., & Randolph, M. F. (2008). Frictionless shear at great depth and other paradoxes of hard rocks. *International Journal of Rock Mechanics and Mining Sciences, 45*(3), 316-328.

Thompson, J. M. T., & Hunt, G. W. (1973). *A general theory of elastic stability*. London; New York: J. Wiley.

Wang, Y. C., & Lakes, R. S. (2004). Exreme stiffness systems due to negative stiffness elements. *American Journal of Physics, 72*(1), 40-50.

Yap, H. W., Lakes, R. S., & Carpick, R. W. (2008). Negative stiffness and enhanced damping of individual multiwalled carbon nanotubes. *Physical Review B, 77*(4).